

An improved interferometer design for use with meteor radars

J. Jones

Department of Physics and Astronomy, University of Western Ontario, London, Ontario, Canada

A. R. Webster

Department of Electrical and Computer Engineering, University of Western Ontario, London, Ontario, Canada

W. K. Hocking

Department of Physics and Astronomy, University of Western Ontario, London, Ontario, Canada

Abstract. The measurement of the directions of radio meteors with an interferometric system is beset by two problems: (1) The ambiguity in the measured directions for antennas spaced by more than $\lambda/2$ and (2) the effects of mutual impedance when the antennas are spaced at $\lambda/2$ and less to avoid these ambiguities. In this paper we discuss the effects of mutual impedance between spaced antennas and describe an interferometer which both minimizes these effects and avoids the ambiguities associated with spacings larger than $\lambda/2$. We have modeled a version of this design numerically and show that under ideal conditions an interferometer of total span 4.5λ can yield directions accurate to about 0.3° with a signal-to-noise ratio of 20 dB. Finally, we have tested the design with observations from the 1996 Geminid and 1997 Quadrantid meteor showers and find that even without a ground plane, the interferometer provides unambiguous directions to an accuracy of the order of 1.5° .

1. Introduction

The measurement of the echo directions of radio meteors is important in several fields of study. Since the reflection process of radio waves from meteor trains is predominantly specular for underdense meteors, the direction of the echo contains important information about the trajectory of the associated meteoroid and the extraction of this directional information has been at the core of most of the methods for deducing the orbits of the meteoroids [Weiss and Elford, 1963; Morton and Jones, 1982; Baggaley et

al., 1993.]. The Doppler shifts of the frequencies of radio-meteor echoes are also routinely used to measure winds in the upper atmosphere [Spizzichino et al., 1965; Roper, 1975; Nakamura et al., 1995; Valentic et al., 1996; Hocking, 1997], and when coupled with range and directional information, this provides a description of the wind field. More recently measurements of the ambipolar diffusion coefficients using the decay times of underdense radio-meteors has enabled the variation of atmospheric temperature with height as determined from the range and elevation of the meteor echo to be monitored on a daily basis [Tsutsumi, et al., 1994; Hocking et al., 1997). Clearly, it is important to be able to measure the echo directions accurately.

Before microcomputers became widely used in data acquisition systems, echo directions were

Copyright 1998 by the American Geophysical Union.

Paper number 97RS03050.
0048-6604/98/97RS-03050\$11.00

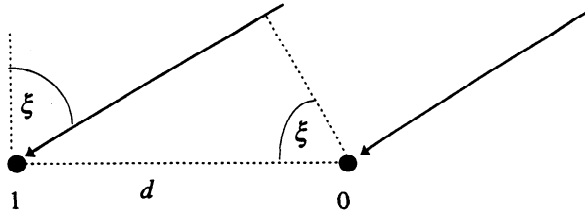


Figure 1. Measurement of angle of arrival, ξ , from the signal phase on spaced antennas.

difficult to measure, and whereas elevations could usually be estimated using range and heights, the azimuth of the echo was usually uncertain to within the width of the antenna beam. Certainly, it was possible to measure directions using the phase differences between elements of an interferometer, but the amount of data reduction required when several antennas were used was daunting. Nowadays this is no longer a problem, and interferometers are used routinely to obtain the directions of meteor echoes.

The use of interferometers, however, has its problems. In order to measure the echo direction unambiguously over the visible hemisphere down to low elevation angles, the antennas of a two-element interferometer must be separated by no more than 0.5λ if no information other than phase is used. If range information is available, it is often possible to resolve this ambiguity, since the meteors usually occur in the height range 80-120 km; but for systems with high pulse-repetition frequencies this may not be possible because of range aliasing. An important consideration is the mutual coupling between the antennas, which increases as their spacing decreases, so that there is the likelihood that the phase difference between the signals from the two antennas is seriously in error.

In this paper we discuss the errors resulting from the effects of mutual coupling of the antennas and show that they cannot be neglected for small antenna spacings. We then present a design for a three-element interferometer which avoids the effects of mutual coupling while at the same time resolves the directional ambiguity. We present the results of numerical experiments

which show that this design can yield very accurate directions, and finally, we present some results of observations of radio meteors using such an interferometer.

2. The Effects of Mutual Coupling on the Measured value of Angle of Arrival using Linearly Spaced Antennas

In principle, the angle of arrival (AOA) of radio waves at a receiving site can be determined by measuring the phase angle difference ϕ_{10} between two antennas spaced by distance d as shown in Figure 1, the angle ξ being measured relative to the normal to the axis of the array. Angular measurements in three dimensions can be obtained from two such arrays arranged orthogonally.

The phase ϕ_{10} of the signal on antenna 1 relative to antenna 0 in Figure 1 is given by,

$$\phi_{10} = -2\pi \frac{d}{\lambda} \sin \xi \quad (1)$$

Since ϕ_{10} is measured in the range $\pm\pi$, the value of ξ is determined unambiguously in the range $\pm\pi/2$ only if $d \leq 0.5\lambda$. On the other hand, larger values of d result in a better estimate of ξ . A common arrangement to accommodate both of these desirable features is an array of several elements spanning a large aperture with adjacent elements spaced $\lambda/2$. A problem does arise, though, with mutual coupling between adjacent closely spaced elements so that the measured value of ϕ can be significantly in error; these mutual coupling effects diminish as the spacing is increased, i.e., as the mutual impedance (Z_m) decreases. For identical antennas (with impedance Z_a in isolation, each connected to matched loads ($Z_L = Z_{in}^*$), the equivalent circuit is shown in Figure 2. Expressions for the calculation of mutual impedance can be found in several standard textbooks [e.g., see Balanis, 1982].

The phase of the currents I_0 and I_1 flowing into the loads are the measured phases, whereas the required phases are those of the open cir-

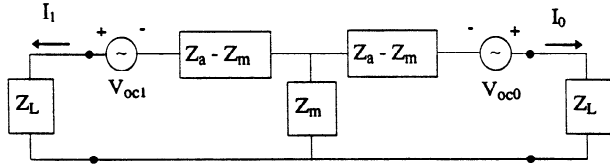


Figure 2. Electrical equivalent circuit for closely spaced identical antennas.

circuit voltages induced in the antennas as given above; it will be noted that if Z_m is zero, then the measured phase is that required.

For two half-wave dipoles spaced $\lambda/2$, as shown in Figure 3, the coupling is significant so that the measured phase (ϕ_{10}) is modified from that which would be obtained in isolation. If this phase is inserted into equation (1), then the inferred value of the angle of arrival is in error, as shown in Figure 4.

Although the collinear arrangement produces the greater error at such close spacing, the mutual impedance decreases much more rapidly with increasing separation than the side-by-side case. The zero error for directions orthogonal to the array axis is always found at any separation, but the zero error along the array axis is only found at separations which are multiples of $\lambda/2$. This is because at angles of arrival close to the axis of the array, the generators are in antiphase at such spacings, and thus the currents are also in antiphase, as may be seen by inspection of Figure 2. At any other spacing, the errors in phase can produce large angular errors for echo directions close to the array axis, since for a given finite phase error, $\Delta\phi_{10}$, the error $\Delta\xi$ in AOA is given by

$$\Delta\xi \approx -\frac{\lambda\Delta\phi_{10}}{2\pi d \cos \xi} \quad (2)$$

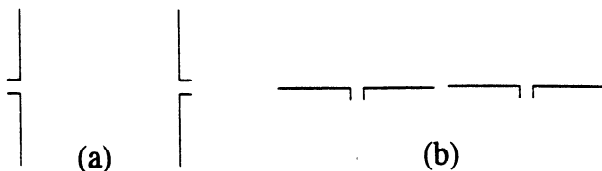


Figure 3. Half-wave dipoles spaced by $\lambda/2$; (a) side by side and (b) collinear.

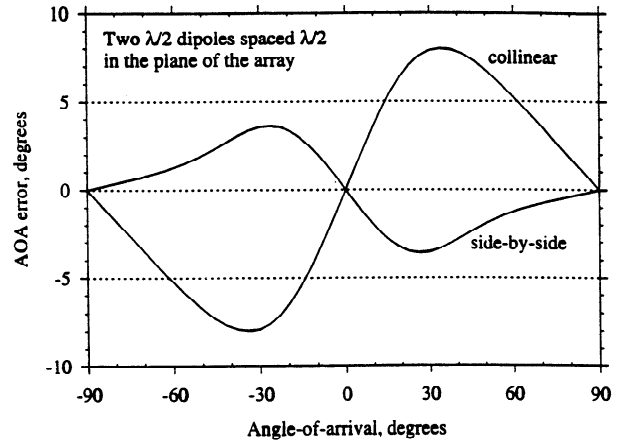


Figure 4. The error in angle of arrival (AOA) for the closely spaced dipoles in Figure 3.

A plot of the error in AOA (i.e., $\Delta\xi$ versus AOA) is shown in Figure 5 for separation in the range $0.5 - 1.0\lambda$. We see that for separation close to 0.75λ , the error increases as the array axis is approached, while the error at large ξ for a separation of 0.5λ and 1.0λ approaches zero as in Figure 4; these phenomena, albeit with diminishing amplitude, are repeated at intervals of $\lambda/2$. As a consequence it is clear that the separation between such dipoles should be set at a multiple of $\lambda/2$ to minimize the angular error at larger values of ξ , and separations of $(2m + 1)\lambda/4$, where m is an integer, should be avoided. In fact, in Figure 5 the range in ξ is restricted to $\pm 65^\circ$ since outside the range $\pm 70^\circ$, the estimate of the true value of ξ is inaccessible due to the errors introduced by the mutual coupling effects. This effect is shown to better advantage in Figure 6, which relates to a spacing of 0.75λ ($m = 1$).

As the separation between antennas increases, the mutual effects diminish, so that for a given acceptable error in the echo direction a suitable spacing may be chosen. Spacings of $n\lambda/2$ are desirable, and Figure 7 shows the errors introduced in measured echo directions due to the mutual coupling effects over the range $0.5-2.5\lambda$. From this, it can be seen that for spacings greater than about 1.5λ , the effects are quite small, with errors less than 0.5° .

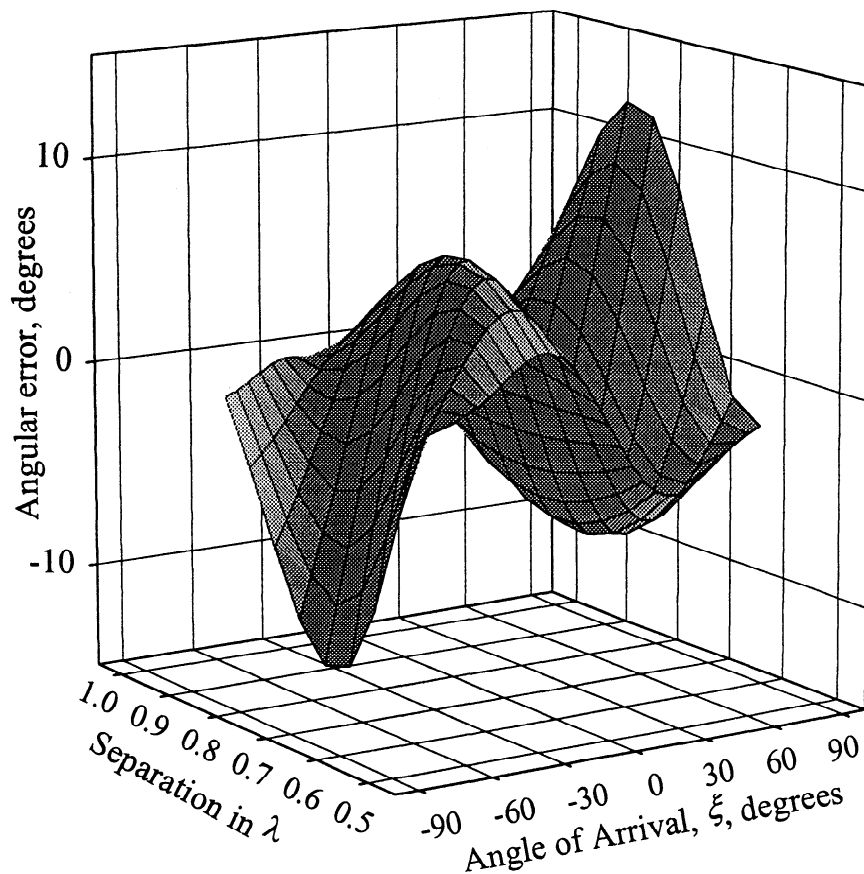


Figure 5. Angular error (in angle-of-arrival) versus angle-of-arrival (range $\pm 65^\circ$ shown for side-by-side dipoles with separation in the range $0.5 - 1.0\lambda$).

3. An Improved Meteor Radar Interferometer

In order to obtain an accurate estimate of the angle of arrival using two spaced antennas it is desirable to use a spacing of several wavelengths, but this introduces ambiguities due to the uncertainty of the number of multiples of 2π introduced. Additional antennas separated by $\lambda/2$ are still needed to resolve these ambiguities, but, as has been shown, the mutual coupling produces significant errors at such close spacing. A solution to this problem is to use three antennas arranged to be spaced by distances differing by $\lambda/2$; for example, in Figure 8, values of $d_1 = 2.5\lambda$ and $d_2 = 2.0\lambda$ might be used. Phase measurements ϕ_{10} and ϕ_{20} relative to the center

antenna then allow unambiguous determination of the angle of arrival since

$$\phi_{10} = -\frac{2\pi d_1}{\lambda} \sin \xi \quad (3)$$

$$\phi_{20} = +\frac{2\pi d_2}{\lambda} \sin \xi \quad (4)$$

so that essentially two estimates of ξ are available:

$$\sin \xi = -\frac{\lambda}{2\pi} \frac{(\phi_{10} - \phi_{20})}{(d_1 + d_2)} \quad (5)$$

$$\sin \xi = -\frac{\lambda}{2\pi} \frac{(\phi_{10} + \phi_{20})}{(d_1 - d_2)} \quad (6)$$

The first giving an accurate, but ambiguous answer, while the second gives a less accurate answer but resolves the ambiguity since $(d_1 - d_2)$

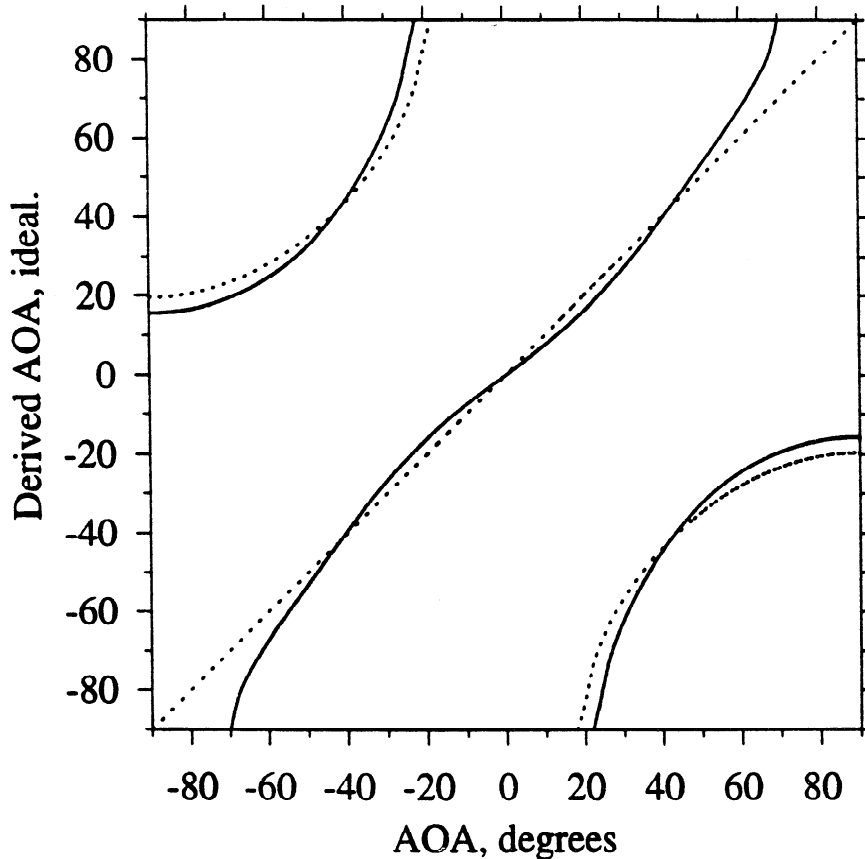


Figure 6. The AOA derived from the phase measurements from side-by-side $\lambda/2$ dipoles spaced by 0.75λ ; the dotted lines are for the ideal case of no mutual coupling effects while the solid lines allow for these effects, and illustrate the errors introduced. Note the fact that for $\xi > \pm 70^\circ$ a good estimate of the AOA is not available.

is equal to $\lambda/2$ and the multiples of 2π cancel in the numerator. For example, with $d_1 = 2.5\lambda$ and $d_2 = 2.0\lambda$ and with $\xi = -40^\circ$, we measure $\phi_{10} = +141.5^\circ$ and $\phi_{20} = +102.8^\circ$ so that the quantities $(\phi_{10} - \phi_{20})$ and $(\phi_{10} + \phi_{20})$ evaluate to -38.7° and -115.7° , respectively. This is illustrated in Figure 9, where the measured phase associated with $(d_1 + d_2)$ gives multiple accurate possibilities from which the correct value of ξ is determined by the measurement associated with $(d_1 - d_2)$. The shaded bands cover a representative phase uncertainty of $\pm 15^\circ$, and the points raised above regarding ambiguities and accuracy are apparent; note that from equation (2), a

phase uncertainty of $\pm 15^\circ$ at $\xi = -40^\circ$ translates into respective errors of $\pm 6^\circ$ and $\pm 0.7^\circ$ for the close and wide spacings in this example.

The uncertainty in the phase measurements is directly affected by the signal-to-noise ratio, and in relation to this, two points are worth noting from Figure 9:

1. As the echo direction becomes closer to the array axis, the phase uncertainty results in a larger uncertainty in the measured echo direction and the echo direction may become indeterminate if the phase uncertainty is too large.

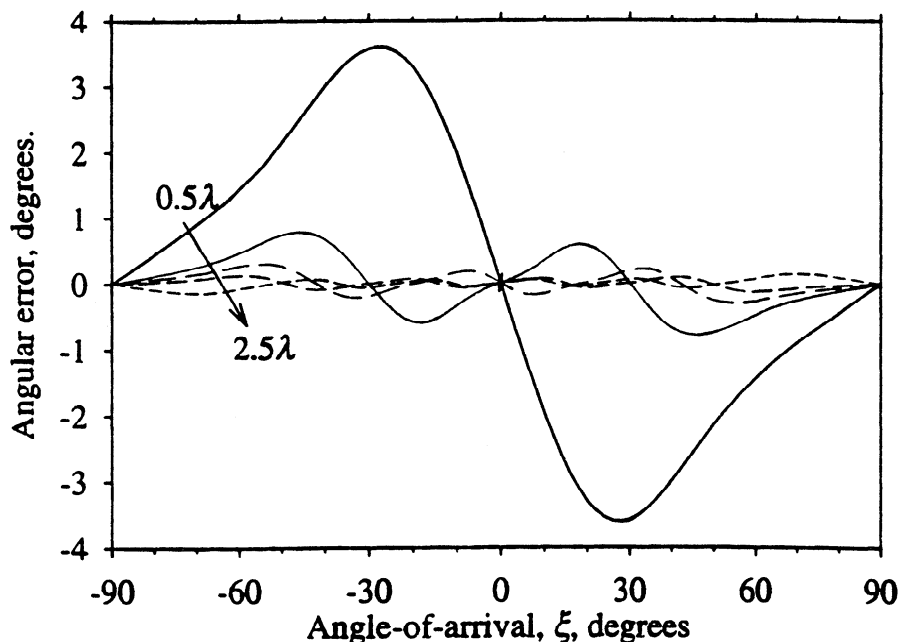


Figure 7. Errors in AOA for side-by-side dipoles with spacings at $\lambda/2$ intervals.

2. The separation of the multiple estimates in the echo directions for the wide spacing must be greater than the uncertainty in the estimate from the close spacing. In other words, it is not practical to extend the separations indefinitely in order to gain a corresponding improvement in accuracy.

Although the first part of this exercise involved only two dipoles, in practice, the situation would be much more complex if the antennas have parasitic elements, particularly in the presence of a nearby ground. Nevertheless, it is apparent that the effects of coupling between

the antennas decrease rapidly as the spacing is increased and are likely to be negligible for spacings greater than 2λ .

4. Numerical Modeling

How well can we expect to measure echo directions using this design of interferometer? In practice, the accuracy will be limited by the signal-to-noise ratio, and in this section we describe the results of numerically modeling the direction-measuring procedure. We take our system to be a five-element interferometer as shown in Figure 10, consisting of two orthogonal three-element linear interferometers with a common central element. For the sake of this study we have supposed the antennas to have isotropic gain, and we have ignored the effects of the ground reflections.

Echo directions were generated with a uniform random distribution in direction, and the resulting inphase (I) and quadrature (Q) signals were calculated for each antenna. Gaussian noise corresponding to a specified mean signal-to-noise

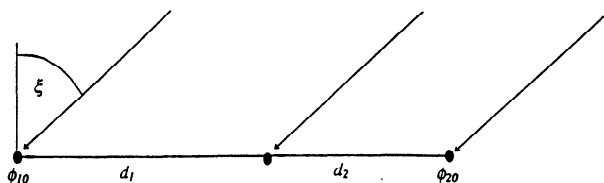


Figure 8. A linear array of three elements with the centre one used as phase reference.

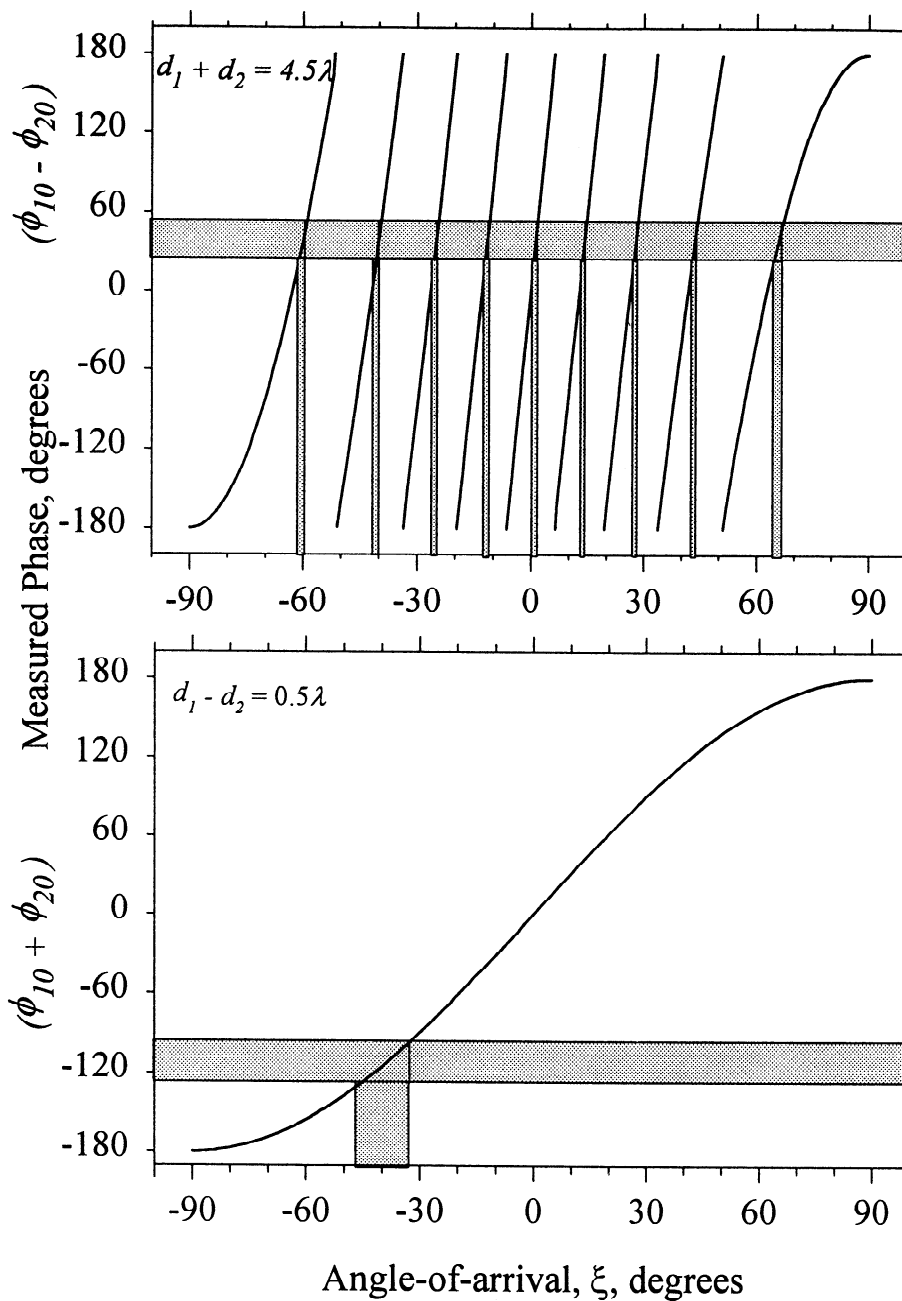


Figure 9. The relationship between the measured phase angles and derived angle of arrival, where the phases are as indicated in Figure 8. The shaded bands show the effect of uncertainties of $\pm 15^\circ$ in the total phases.

ratio was then added to each of the I and Q signals and the resultant phase calculated. We then were able to calculate the apparent direction cosines to each of the interferometer axes

using equation (6) to get an initial estimate and then refining it using equation (5). For each of these trials the angle between the original and apparent directions were calculated, and a plot

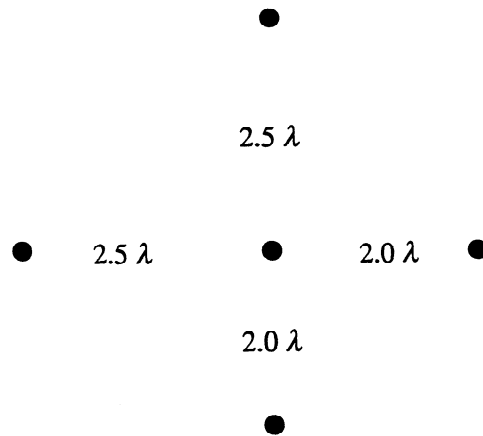


Figure 10. Interferometer configuration for the numerical model.

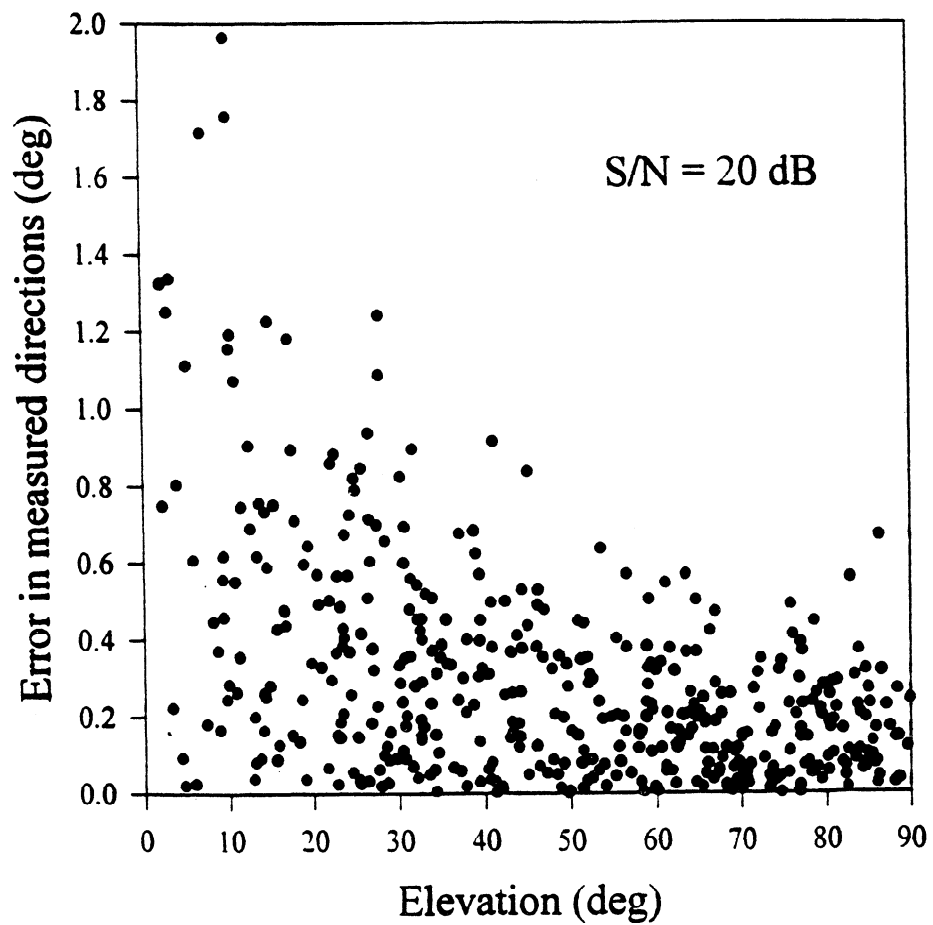


Figure 11. Error in direction as a function of angle of elevation for numerical model. Note that the elevation angle is derived from the angle of arrival ξ used earlier.

of these directional errors as a function of echo elevation for one such numerical experiment involving 500 trials in which the mean signal-to-noise ratio was 20 dB is shown in Figure 11.

The mean error in directions for elevations above 30° is 0.31° . For smaller elevations the error increases rapidly with decreasing elevation angle; for example, at an elevation of 20° the average error in the directions is about 1.8° . We have investigated the model at length and find, as would be expected, that increasing the signal to noise ratio improves the measurements even more: Doubling the signal-to-noise ratio to 26 dB reduces the error in direction by approximately a factor of 2. There seems to be little advantage in increasing the antenna spacing, but the accuracy can be increased by an order of magnitude by adding two extra antennas spaced at, say, 30λ from the center. We have also modeled the situation with smaller signal-to-noise ratios and find that below 17 dB the method starts to produce grossly incorrect apparent echo directions even for elevations greater than 30° , but the fraction of these is small even for signal-to-noise ratios as small as 10 dB. This, of course, applies only to the case when a single phase measurement is made at each antenna; when several measurements are available which can be averaged, the accuracy is improved accordingly.

5. Observational Results.

We have incorporated a five-element interferometer similar to that used in the model above into the Canadian London Ontario VHF atmospheric radar (CLOVAR) located at 43°N , 81°W , which has been described by *Hockins* [1997]. The end antennas were placed at 2.0 and 2.5λ from the central antenna as in the model, but whereas the model did not have to include the effects of the ground, the actual interferometer was built on uneven terrain and was also close to some trees, both of which introduce phase errors whose magnitude it is difficult to estimate. The performance of the interferometer was investigated using observations made

with CLOVAR in its meteor mode during the Geminid and Quadrantid meteor showers in December 1996 and January 1997, respectively.

We estimated the directional errors using two methods: (1) from the residual phase error after the signal direction was determined and (2) from the apparent scatter in the directions of echoes belonging to meteor showers. The first method indicated that the measurement error in direction is approximately 2° for echoes with elevations greater than 30° .

Shower meteors (Geminids and Quadrantids, in this case) have essentially parallel trajectories, and the specular reflection condition dictates that the echo directions are perpendicular to this direction. We were therefore able to select those meteors which fulfilled this condition to within a specified tolerance, $\pm\theta$, and Figure 12 shows how the number of such meteors varied with θ . For a Gaussian distribution in signal direction resulting from a small dispersion in the directions of the meteor trajectories, as well as measurement errors in the echo directions, the number N of echoes satisfying a given specular tolerance condition is given approximately by

$$N = A \operatorname{erf}(\theta/\sqrt{2}\sigma) + B\theta \quad (7)$$

where σ is the composite dispersion in the echo directions and the linear term is to take account of contamination by sporadic meteors which becomes more severe as θ increases. The coefficients A and B are proportional to the shower and sporadic activity. We have verified that this approximation is valid and that accurate values of σ are obtained by using a least squares method to fit this formula to with simulated data. Applying this method to the observational Geminid and Quadrantid data, we find that the apparent scatter in echo directions is 1.5° and 1.7° , which represents an upper limit to the measurement error since it also incorporates the intrinsic scatter in the meteoroid trajectories, which is probably the reason that the scatter is somewhat greater for the Quadrantids than for the Geminids.

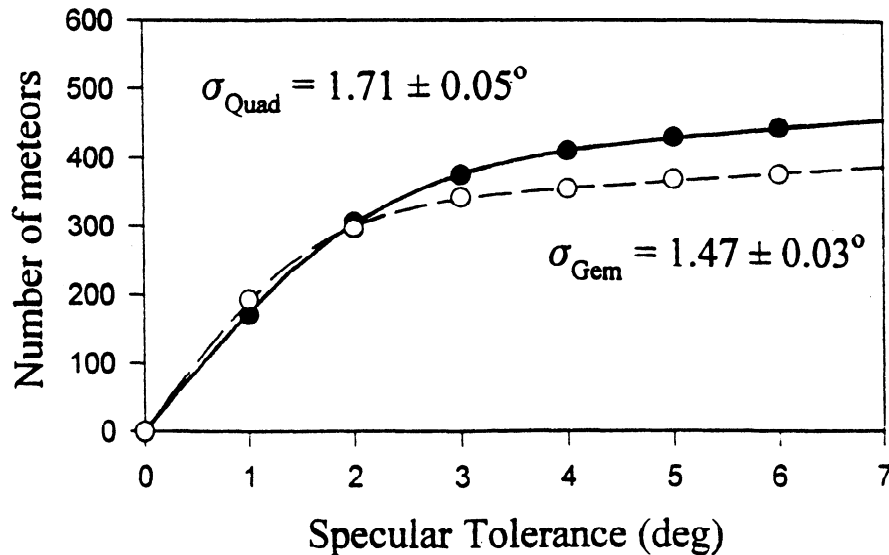


Figure 12. Fit of equation (7) to observational data to obtain apparent scatter in echo direction. Solid circles indicate Quadrantids 1997, and open circles indicate Geminids 1996.

The value of $\pm 1.5^\circ$ obtained observationally is much greater than the 0.31° accuracy that the method is capable of, and we attribute the difference to the effects of uneven terrain and trees. It is clear that care must be taken to reduce such effects to realize the potential accuracy of the interferometer, and this may take the form of a carefully constructed ground plane or the use of antennas with polar diagrams that minimize ground reflections. For many applications such heroic efforts are not warranted, and it is sufficient to measure directions to an accuracy of a degree or two without the worry of possible ambiguities.

Acknowledgments. The authors gratefully acknowledge the funding of this project by the National Science and Engineering Research Council of Canada.

References

- Baggaley, W.J., A.D. Taylor, and D.I. Steel, The Southern Hemisphere Meteor Orbit Radar facility: AMOR, in *Meteoroids and their Parent Bodies*, edited by J. Stohl and I.P. Williams. pp. 245-248, 1993. Atron. Inst. of the Slovak Acad. of Sci., Bratislava.
- Balanis, C.A., *Antenna Theory - Analysis and Design*, Harper Collins, New York, 1982.
- Hocking, W. K., System design, signal-processing procedures and preliminary results for the Canadian (London, Ontario) VHF atmospheric radar, *Radio Sci.*, 32 (2) 687-706, 1997.
- Hocking, W. K., T. Thayaparan, and J. Jones., Meteor decay times and their use in determining a diagnostic mesospheric temperature-pressure parameter: Methodology and 1 year of data. *Geophys. Res. Lett.*, 24, 2977-2980, 1997.
- Morton, J. D., and J. Jones., A method for imaging radio meteor radiant distributions. *Mon. Not. R. Astron. Soc.*, 198, 737-746, 1982.
- Nakamura, T., T. Tsuda, and M. Tsutsumi, Meteor wind observations with the MU radar., *Radio Sci.*, 26 (4) 857-869, 1991.
- Roper, R. G., The measurement of meteor winds over Atlanta., *Radio Sci.*, 10 (3) 363-369, 1975.
- Spizzichino, A., J. Delcourt, A. Giraud, and I. Revah, A new type of continuous wave radar for the observation of meteor trails, *Proc. IEEE*, 53, 1084-1086, 1965.
- Tsutsumi, M., T. Tsuda, T. Nakamura, and S. Fukao, Temperature fluctuations near the mesopause inferred from meteor observations with the middle and upper atmosphere radar, *Radio Sci.*, 29 (3), 599-610, 1994.
- Valentic, A., J. P. Avery, S. K. Avery, M. A. Cervera, W. G. Elford, R. A. Vincent, and I. M. Reid. A comparison of meteor radar systems at Buckland Park, *Radio Sci.*, 31 (6) 1313-1329, 1996.
- Weiss, A. A., and W. G. Elford, An equipment for combined geophysical and astronomical measurements of meteors., *Proc. Inst. Radio Eng. Aust.*, 24 197, 1963.

W. K. Hocking and J. Jones Department of Physics and Astronomy, University of Western Ontario, London, Ontario, Canada. N6A 3K7 (e-mail: whocking@danlon.physics.uwo.ca; jim.jones@julian.uwo.ca)

A. R. Webster, Department of Electrical and Computer Engineering, University of Western Ontario, London, Ontario, Canada. N6A 5B9 (e-mail: awebster@engntadmin.engga.uwo.ca)

Received June 23, 1997; revised October 21, 1997; accepted October 29, 1997)